

Algorithm Selection for Deep Active Learning with Imbalanced Datasets

Jifan Zhang^{1*} Shuai Shao² Saurabh Verma² Robert Nowak¹

Abstract

Label efficiency has become an increasingly important objective in deep learning applications. Active learning aims to reduce the number of labeled examples needed to train deep networks, but the empirical performance of active learning algorithms can vary dramatically across datasets and applications. It is difficult to know in advance which active learning strategy will perform well or best in a given application. To address this, we propose the first adaptive algorithm selection strategy for deep active learning. For any unlabeled dataset, our (meta) algorithm TAILOR (Thompson ActIve Learning algORithm selection) iteratively and adaptively chooses among a set of candidate active learning algorithms. TAILOR uses novel reward functions aimed at gathering class-balanced examples. Extensive experiments in multi-class and multi-label applications demonstrate TAILOR’s effectiveness in achieving accuracy comparable or better than that of the best of the candidate algorithms.

1. Introduction

Active learning (AL) aims to reduce data labeling cost by iteratively and adaptively finding informative unlabeled examples for annotation. Label-efficiency is increasingly crucial as deep learning models require large amount of labeled training data. In recent years, numerous new algorithms have been proposed for deep active learning (Sener & Savarese, 2017; Gal et al., 2017; Ash et al., 2019; Kothawade et al., 2021; Citovsky et al., 2021; Zhang et al., 2022). Relative label efficiencies among algorithms, however, vary significantly across datasets and applications (Beck et al., 2021; Zhan et al., 2022). When it comes to choosing the best algorithm for a novel dataset or application, practitioners have been mostly relying on educated guesses and subjective preferences. In this work, we present

*Work done at Meta. ¹University of Wisconsin, Madison, USA ²Meta, Menlo Park, USA. Correspondence to: Jifan Zhang <jifan@cs.wisc.edu>.

a principled approach for automatically selecting effective deep AL algorithms for novel, unlabeled datasets.

Prior to the wide adoption of neural network models, Baram et al. (2004); Hsu & Lin (2015); Pang et al. (2018) studied the online choice of active learning algorithms for linear models. The general approach is to reduce the algorithm selection task to a multi-armed bandit problem. As shown in Figure 1, the idea may be viewed as a meta algorithm that adaptively chooses among a set of candidate AL algorithms (arms). The objective of the meta algorithm is to maximize the cumulative reward incurred from running the chosen candidate algorithms. Previous works have proposed various generalization error surrogates as reward functions, but these are problematic in deep active learning settings. To compute reward, Baram et al. (2004) requires model retraining for every newly labeled example, which is computationally prohibitive for deep learning models. Hsu & Lin (2015) and Pang et al. (2018) propose to utilize training accuracy as part of their rewards, which becomes ineffective due to universal approximation of neural networks.

In Section 3 of this paper, we first present a general framework of online AL algorithm selection that encompasses problem settings of Baram et al. (2004); Hsu & Lin (2015); Pang et al. (2018). In Section 4, we then propose reward functions that encourage the collection of *class-balanced* labeled set. For example, one reward is defined as a weighted sum over number of labeled examples collected from each class, where rarer classes are up-weighted to encourage *class diversity*. To accommodate these reward functions, we reduce the meta algorithm to a novel bandit problem (Section 4.2) and propose a novel Thompson Sampling (Thompson, 1933) style algorithm TAILOR (Section 4.3). In Section 5, we provide regret analysis and compare against a Thompson Sampling algorithm for linear contextual bandit (Russo & Van Roy, 2014).

To highlight our key contributions in this paper:

- To our knowledge, we propose the first adaptive algorithm selection strategy for *deep* active learning. Our algorithm TAILOR works particularly well on the challenging and prevalent class-imbalance settings (Kothawade et al., 2021; Emam et al., 2021; Zhang et al., 2022).
- Our framework is general purpose for both multi-label and multi-class classification. Active learning is espe-

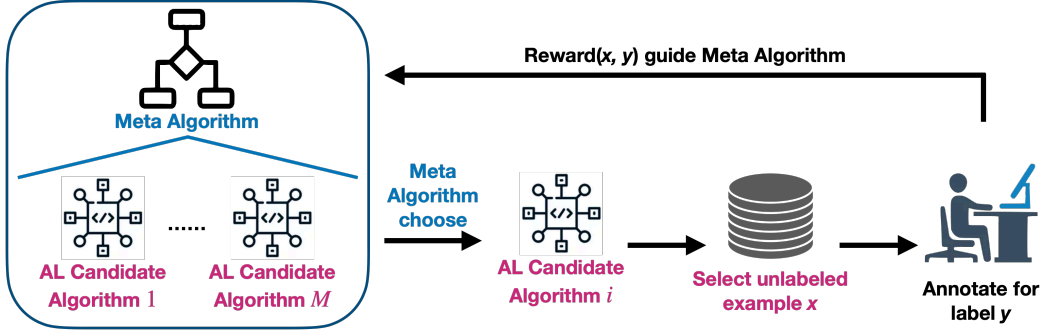


Figure 1. Adaptive active learning algorithm selection framework for batch size 1. Our framework proposed in Section 3.2 is a batched version that chooses multiple candidate algorithms and unlabeled examples every iteration. The labels and rewards are all revealed at once in the end of the iteration.

cially helpful for multi-label classification due to the high annotation cost of obtaining *multiple* labels for each example.

- TAILOR can choose among large number (e.g. hundreds) of candidate deep AL algorithms even under limited (10 or 20) rounds of interaction. This is particularly important since limiting the number of model retraining steps and training batches is essential in large-scale deep active learning (Citovsky et al., 2021).
- We provide extensive experiments on four multi-label and five multi-class image classification datasets (Section 6). Our results show that TAILOR obtains accuracies comparable or better than the best candidate strategy for eight out of the nine datasets. On all of the nine datasets, TAILOR succeeds in collecting datasets as class-balanced as the best candidate algorithm. Moreover, with a slightly different reward function designed for active search, TAILOR performs the best in finding the highest number of positive class labels on all multi-label datasets.

2. Related Work

Adaptive Algorithm Selection in Active Learning. Several past works have studied the adaptive selection of active learning algorithms for linear models. Donmez et al. (2007) studied the limited setting of switching between two specific strategies to balance between uncertainty and diversity. To choose among off-the-shelf AL algorithms, Baram et al. (2004) first proposed a framework that reduced the AL algorithm selection task to a multi-armed bandit problem. That approach aims to maximize the cumulative reward in a Classification Entropy Maximization score, which measures the class-balancedness of predictions on unlabeled examples, after training on each newly labeled example. However, this becomes computationally intractable for large datasets with computationally expensive models. To remedy this problem, Hsu & Lin (2015) and Pang et al. (2018) proposed the use of importance weighted training accuracy scores for each

newly labeled example. The training accuracy, however, is almost always 100% for deep learning models due to their universal approximation capability, which makes the reward signals less effective. Moreover, Hsu & Lin (2015) reduced their problem to an adversarial multi-armed bandit problem while Pang et al. (2018) also studied the non-stationarity of rewards over time.

Lastly, we would like to distinguish the goal of our paper from the line of *Learning Active Learning* literature (Konyushkova et al., 2017; Shao et al., 2019; Zhang et al., 2020; Gonsior et al., 2021; Löffler & Mutschler, 2022), where they learn a single parameterized policy model from offline datasets. These policies can nonetheless serve as individual candidate algorithms, while TAILOR aims to select the best subsets that are adapted for novel dataset instances.

Multi-label Deep Active Learning. Many active learning algorithms for multi-label classification based on linear models have been proposed (Wu et al., 2020), but few for deep learning. Multi-label active learning algorithms are proposed for two types of annotation, *example-based* where all associated labels for an example are annotated, and *example-label-based* where annotator assigns a binary label indicating whether the example is positive for the specific label class.

While Citovsky et al. (2021); Min et al. (2022) both propose deep active learning algorithms for example-label-based labels, we focus on example-based annotation in this paper. To this end, Ranganathan et al. (2018) propose an uncertainty sampling algorithm that chooses examples with the lowest class-average cross entropy losses after trained with weak supervision. We find the EMAL algorithm by Wu et al. (2014) effective on several datasets, despite being proposed for linear models. EMAL is based on simple uncertainty metric where one averages over binary margin scores for each class. Lastly, a multi-label task can be seen as individual single-label binary classification tasks for each class (Boutell et al., 2004). By adopting this view, one can ran-

domly interleave the above-mentioned AL algorithms for every class. In this paper, we include baselines derived from least confidence sampling (Settles, 2009), GALAXY (Zhang et al., 2022) and most likely positive sampling (Warmuth et al., 2001; 2003; Jiang et al., 2018).

Balanced Multi-class Deep Active Learning. Traditional uncertainty sampling algorithms have been adopted for deep active learning. These algorithms select uncertain examples based on scores derived from likelihood softmax scores, such as margin, least confidence and entropy (Tong & Koller, 2001; Settles, 2009; Balcan et al., 2006; Kremer et al., 2014). The latter approaches leverage properties specific to neural networks by measuring uncertainty through dropout (Gal et al., 2017), adversarial examples (Ducoffe & Precioso, 2018) and neural network ensembles (Beluch et al., 2018). Diversity sampling algorithms label examples that are most different from each other, based on similarity metrics such as distances in penultimate layer representations (Sener & Savarese, 2017; Geifman & El-Yaniv, 2017; Citovsky et al., 2021) or discriminator networks (Gissin & Shalev-Shwartz, 2019). Lastly, gradient embeddings, which encode both softmax likelihood and penultimate layer representation, have become widely adopted in recent approaches (Ash et al., 2019; 2021; Wang et al., 2021; Elenter et al., 2022; Mohamadi et al., 2022). As an example, Ash et al. (2019) uses a k-means++ algorithm to query a diverse set of examples in the gradient embedding space.

Unbalanced Multi-class Deep Active Learning. More general and prevalent scenarios, such as unbalanced deep active classification, have received increasing attention in recent years (Kothawade et al., 2021; Emam et al., 2021; Zhang et al., 2022; Coleman et al., 2022; Jin et al., 2022; Aggarwal et al., 2020; Cai, 2022). For instance, Kothawade et al. (2021) label examples with gradient embeddings that are most similar to previously collected rare examples while most dissimilar to out-of-distribution ones. Zhang et al. (2022) create linear one-vs-rest graphs based on margin scores. To collect a more class-diverse labeled set, GALAXY discovers and labels around the optimal uncertainty thresholds through a bisection procedure on shortest shortest paths.

3. Problem Statement

3.1. Notation

In pool based active learning, one starts with a large pool of N unlabeled examples $X = \{x_1, x_2, \dots, x_N\}$ with corresponding ground truth labels $Y = \{y_1, y_2, \dots, y_N\}$ initially unknown to the learner. Let K denote the total number of classes. In multi-label classification, each label y_i is denoted as $y_i \in \{0, 1\}^K$ with each element $y_{i,j}$ representing the binary association between class j and example x_i .

On the other hand, in a multi-class problem, each label $y_i \in \{e_j\}_{j \in [K]}$ is denoted by a canonical one-hot vector, where e_j is the j -th canonical vector representing the j -th class. Furthermore, at any time, we denote labeled and unlabeled examples by $L, U \subset X$ correspondingly, where $L \cap U = \emptyset$. Lastly, let $L_0 \subset X$ denote a small seed set of labeled examples and $U_0 = X \setminus L_0$ denote the initial unlabeled set.

3.2. Adaptive Algorithm Selection Framework

In this section, we describe a generic framework that encompasses the online algorithm selection settings in Baram et al. (2004), Hsu & Lin (2015) and Pang et al. (2018). As shown in Algorithm 1, at each iteration, a meta algorithm chooses a multi-set of candidate AL algorithms. Then a batch of examples are selected according to this multi-set and labeled. The meta algorithm aims to maximize the future cumulative reward based on noisy past reward observations of each candidate algorithm. The reward function $r : X \times Y \rightarrow \mathbb{R}$ is measured based on an algorithm's selected examples and corresponding labels. There are two key components to this framework: the choice of reward function and a bandit strategy that uses the rewards optimize algorithm selection. Our particular design will be presented in Section 4.

Formally, an active learning algorithm \mathcal{A} takes as input a pair of labeled and unlabeled sets (L, U) and returns an unlabeled example $\mathcal{A}(L, U) \in U$. As shown in Algorithm 1, the meta algorithm has access to M such candidate algorithms $A = \{\mathcal{A}_1, \dots, \mathcal{A}_M\}$. At the beginning of any round t , B algorithms indexed by $\{\alpha^{t,j}\}_{j=1}^B \in [M]^B$ are chosen. This is a multiset and any one algorithm may appear multiple times in the set. One example is selected by each algorithm in the multiset. This is done sequentially over the multiset without replacement, resulting in a total of B unique examples which are then labeled. At the end of the round, their corresponding rewards $\{r^{t,j}\}_{j=1}^B$ are observed based on the newly annotated examples $\{(x^{t,j}, y^{t,j})\}_{j=1}^B$ selected by these algorithms. The model is also retrained using this batch of examples before proceeding to the next round.

We make the following two crucial assumptions for our framework:

Assumption 3.1. Any candidate batch active learning algorithm \bar{A} can be decomposed into an iterative selection procedure A that returns one unlabeled example at a time.

The assumption has been inherently made by our framework above where an active learning algorithm returns one unlabeled example at a time. It entails that running \bar{A} once to collect a batch of B examples is equivalent with running the iterative algorithm A for B times. As noted in Appendix A.1, most existing deep active learning algorithms can be decomposed into iterative procedures and thus

Algorithm 1 General Meta Active Learning Framework for Baram et al. (2004); Hsu & Lin (2015); Pang et al. (2018)

Define: M candidate algorithms $A = \{\mathcal{A}_i\}_{i \in [M]}$, pool X , total number of rounds T , fixed batch size B .

Initialize: Labeled seed set $L_0 \subset X$, unlabeled set $U_0 = X \setminus L_0$ and initial policy Π^1 .

for $t = 1, \dots, T$ **do**

- Meta algorithm Π^t chooses multiset of algorithms $\mathcal{A}_{\alpha_{t,1}}, \mathcal{A}_{\alpha_{t,2}}, \dots, \mathcal{A}_{\alpha_{t,B}}$, where indexes $\alpha_{t,1}, \dots, \alpha_{t,B} \in [M]$.
- Initialize selection set $S_t \leftarrow \emptyset$.
- for** $j = 1, \dots, B$ **do**

 - Run algorithm to select unlabeled example $x^{t,j} := \mathcal{A}_{\alpha_{t,j}}(L_{t-1}, U_{t-1} \setminus S_t)$ that is not yet selected.
 - Insert the example $x^{t,j}$: $S_t \leftarrow S_t \cup \{x^{t,j}\}$.

- end for**
- Annotate $\{x^{t,j}\}_{j=1}^B$ and observe labels $\{y^{t,j}\}_{j=1}^B$.
- Update sets $L_t \leftarrow L_{t-1} \cup S_t$, $U_t \leftarrow U_{t-1} \setminus S_t$.
- Retrain model on L_t to inform the next round.
- Observe reward $r^{t,j} = r(x^{t,j}, y^{t,j})$ for each algorithm $\mathcal{A}_{\alpha_{t,j}}$, where $j \in [B]$.
- Update meta policy statistics based on $x^{t,j}, y^{t,j}$ and $r^{t,j}$ to obtain Π^{t+1} , which informs the next round.

end for

Objective: Maximize cumulative reward $\sum_{t=1}^T \sum_{j=1}^B r^{t,j}$.

can serve as candidate algorithms in our framework.

Assumption 3.2. For each round $t \in [T]$, we assume there exist ground truth reward distributions $\mathbb{P}_{t,1}, \dots, \mathbb{P}_{t,M}$ for each candidate algorithm. Furthermore, for each element $j \in [B]$ in the batch, we make the iid assumption that reward $r^{t,j} \stackrel{iid}{\sim} \mathbb{P}_{t,\alpha_{t,j}}$ is sampled from the distribution of the corresponding selected algorithm.

The iid assumption is made for theoretical simplicity by all of Baram et al. (2004); Hsu & Lin (2015); Pang et al. (2018). We say the distributions are *non-stationary* if for any $i \in [M]$, $P_{t,i}$ varies with respect to time t . Both this paper and Pang et al. (2018) study *non-stationary* scenarios, whereas Baram et al. (2004) and Hsu & Lin (2015) assume the distributions are *stationary* across time.

4. Thompson Active Learning Algorithm Selection

As mentioned in Section 3.2, we present the two key components of our design, reward function and bandit strategy. In Section 4.1, we first present a class of reward functions designed for deep active learning under class imbalance. In Section 4.2, by leveraging the structure of such reward functions, we reduce the adaptive algorithm selection framework

from Section 3.2 into a novel bandit setting. In Section 4.3, we then propose our algorithm TAILOR which is specifically designed for this setting.

4.1. Reward Function

We propose reward functions that encourage selecting examples so that every class is well represented in the labeled dataset, ideally equally represented or “class-balanced”. Our reward function works well even under practical scenarios such as limited number of rounds and large batch sizes (Citovsky et al., 2021). The rewards we propose can be efficiently computed example-wise as opposed to Baram et al. (2004) and are more informative and generalizable than Hsu & Lin (2015) and Pang et al. (2018). Specifically, we focus on the class-balance of the collected labels. Such rewards are especially effective for datasets with underlying class imbalance. Recall $y \in \{0, 1\}^K$ for multi-label classification and $y \in \{e_i\}_{i=1}^K$ for multi-class classification. We define the following types of reward functions.

- **Class Diversity:** To encourage better class diversity, we propose a reward that inversely weights each class by the number of examples already collected. For each round $t \in [T]$,

$$r_{div}^t(x, y) = \frac{1}{K} \sum_{i=1}^K \frac{1}{1 \vee \text{COUNT}^t(i)} y_{:i} =: \langle v_{div}^t, y \rangle$$

where $\text{COUNT}^t(i)$ denotes the number of examples in class i after $t - 1$ rounds and $y_{:i}$ denotes the i -th element of y . We let v_{div}^t denote the inverse weighting vector.

- **Multi-label Search:** As shown in Table 1, multi-label classification datasets naturally tend to have sparse labels (more 0’s than 1’s in y). Therefore, it is often important to search for positive labels. To encourage this, we define a stationary reward function for multi-label classification:

$$r_{search}(x, y) = \frac{1}{K} \sum_{i=1}^K y_{:i} =: \langle v_{pos}, y \rangle$$

where $v_{pos} = \frac{1}{K} \vec{1}$.

- **Domain Specific:** Lastly, we would like to note that domain experts can define specialized weighting vectors of different classes $v_{dom}^t \in [-\frac{1}{K}, \frac{1}{K}]^K$ that are adjusted over time t . The reward function simply takes the form $r_{dom}^t(x, y) = \langle v_{dom}^t, y \rangle$. As an example of multi-label classification of car information, one may prioritize classes of car brands over classes of car types, thus weighting each class differently. They can also adjust the weights over time based on their need.

4.2. Novel Bandit Setting

We now present a novel bandit reduction that mirrors the adaptive algorithm selection framework under this novel

class of rewards. In this setup, $v_t \in [-\frac{1}{K}, \frac{1}{K}]^K$ is arbitrarily chosen and non-stationary. On the other hand, for each candidate algorithm $\mathcal{A}_i \in A$, we assume the labels y are sampled iid from a stationary 1-sub-Gaussian distribution \mathbb{P}_{θ^i} with mean θ^i . Both the stationary assumption in P_{θ^i} and the iid assumption are made for simplicity of our theoretical analysis only. We will describe our implementation to overcome the non-stationarity in \mathbb{P}_{θ^i} in Section 6.1. Although we make the iid assumption analogous to Assumption 3.2, we demonstrate the effectiveness of our algorithm in Section 6 through extensive experiments. Additionally, note that $\theta^i \in [0, 1]^K$ for multi-label classification and $\theta^i \in \Delta^{(K-1)}$ takes value in the K dimensional probability simplex for multi-class classification. In our bandit reduction, at each round t ,

1. Nature reveals weighting vector v^t ;
2. Meta algorithm chooses algorithms $\alpha^{t,1}, \dots, \alpha^{t,B}$;
3. After sequentially collecting unlabeled examples, annotate to observe $y^{t,1}, \dots, y^{t,B}$, where each $y^{t,j} \stackrel{iid}{\sim} \mathbb{P}_{\theta^{\alpha_{t,j}}}$;
4. Objective: maximize rewards defined as $r^{t,j} = \langle v^t, y^{t,j} \rangle$.

This setting bears resemblance to a linear contextual bandit problem. Indeed, one can formulate such a problem close to our setting by constructing arms $\phi_i^t = \text{vec}(v^t e_i^\top) \in [-\frac{1}{K}, \frac{1}{K}]^{KM}$. Here, $\text{vec}(\cdot)$ vectorizes the outer product between v^t and the i -th canonical vector e_i . A contextual bandit algorithm observes reward $r = \langle \phi_i^t, \theta^* \rangle + \varepsilon$ after pulling arm i , where $\theta^* = \text{vec}([\theta^1, \theta^2, \dots, \theta^M]) \in [0, 1]^{KM}$ and ε is some sub-Gaussian random noise. However, this contextual bandit formulation does not take into account the observations of $\{y^{t,j}\}_{j=1}^B$ at each round, which are direct realizations of $\theta^1, \dots, \theta^M$. In fact, standard contextual bandit algorithms usually rely on least squares estimates of $\theta^1, \dots, \theta^M$ based on the reward signals (Russo & Van Roy, 2014). As will be shown in Proposition 5.1, a standard Bayesian regret upper bound from Russo & Van Roy (2014) is of order $\tilde{O}(BM^{\frac{3}{4}}K^{\frac{3}{4}}\sqrt{T})$. Our algorithm TAILOR, on the other hand, leverages the observations of $y^{t,j} \sim \mathbb{P}_{\theta^{\alpha_{t,j}}}$ and has regret upper bounded by $\tilde{O}(B\sqrt{MT})$ (Theorem 5.2), similar to a stochastic multi-armed bandit.

4.3. TAILOR

We are now ready to present TAILOR, a Thompson Sampling style meta algorithm for adaptively selecting active learning algorithms. The key idea is to maintain posterior distributions for $\theta^1, \dots, \theta^M$. As shown in Algorithm 2, at the beginning we utilize uniform priors $\text{Unif}(\Omega)$ over the support Ω , where $\Omega = \Delta^{(t-1)}$ and $[0, 1]^K$ respectively for multi-label and multi-class classification. We note that the choice of uniform prior is made so that it is general purpose for any dataset. In practice, one may design more task-specific priors.

Algorithm 2 TAILOR : Thompson Active Learning Algorithm Selection

Input: M candidate algorithms $A = \{\mathcal{A}_i\}_{i \in [M]}$, pool X , total number of rounds T , fixed batch size B .

Initialize: For each $i \in [M]$, $a^i = b^i = \vec{1} \in \mathbb{R}^{+^K}$.

for $t = 1, \dots, T$ **do**

Nature reveals $v^t \in [-\frac{1}{K}, \frac{1}{K}]^K$

Choose candidate algorithms:

for $j = 1, \dots, B$ **do**

if Multi-class Classification **then**

For each $i \in [M]$, $\hat{\theta}^i \sim \text{Dir}(a^i)$.

else if Multi-label Classification **then**

For each $i \in [M]$, $\hat{\theta}^i \sim \text{Beta}(a^i, b^i)$.

end if

Choose $\alpha^{t,j} \leftarrow \arg \max_{i \in [M]} \langle v^t, \hat{\theta}^i \rangle$.

end for

Run chosen algorithms to collect batch:

for $j = 1, \dots, B$ **do**

Run algorithm $\mathcal{A}_{\alpha^{t,j}}$ to select unlabeled example $x^{t,j}$ and insert into S_t .

end for

Annotate examples in S_t to observe $y^{t,j}$ for each $j \in [B]$.

Update posterior distributions:

For each algorithm $i \in [M]$:

$$a^i \leftarrow a^i + \sum_{j: \alpha^{t,j} = i} y^{t,j}, \quad b^i \leftarrow b^i + \sum_{j: \alpha^{t,j} = i} (1 - y^{t,j}).$$

Retrain neural network to inform next round.

end for

Over time, we keep an posterior distribution over each ground truth mean θ^i for each algorithm $i \in [M]$. With a uniform prior, the posterior distribution is an instance of either element-wise Beta distribution¹ for multi-label classification or Dirichlet distribution for multi-class classification. During each round t , we draw samples from the posteriors, which are then used to choose the best action (i.e., candidate algorithm) that has the largest predicted reward. After the batch of B candidate algorithms are chosen, we then sequentially run each algorithm to collect the batch of unlabeled examples. Upon receiving the batch of annotations, we then update the posterior distribution for each algorithm using the labels. Lastly, the neural network model retrained after the entire batch has been annotated.

5. Analysis

In this section, we present regret upper bound of TAILOR and compare against a linear contextual bandit upper bound

¹For $z \in [0, 1]^d$ and $a, b \in \mathcal{Z}^{+^d}$, we say $z \sim \text{Beta}(a, b)$ if for each $i \in [d]$, $z_i \sim \text{Beta}(a_i, b_i)$.

from Russo & Van Roy (2014). Our time complexity analysis can be found in Appendix C.

Given an algorithm π , the *expected regret* measures the difference between the expected cumulative reward of the optimal action and the algorithm's action. Formally for any fixed instance with $\Theta = \{\theta^1, \dots, \theta^M\}$, the *expected regret* is defined as

$$R(\pi, \Theta) := \mathbb{E} \left[\sum_{t=1}^T \sum_{j=1}^B \max_{i \in [M]} \langle v^t, \theta^i - \theta^{\alpha^{t,j}} \rangle \right]$$

where the expectation is taken over the randomness of the algorithm, e.g. posterior sampling in TAILOR.

Bayesian regret simply measures the average of expected regret over different instances

$$BR(\pi) := \mathbb{E}_{\theta^i \sim \mathbb{P}_0(\Omega), i \in [M]} [R(\pi, \{\theta^i\}_{i=1}^M)]$$

where Ω denotes the support of each θ^i and $\mathbb{P}_0(\Omega)$ denotes the prior. Recall $\Omega = [0, 1]^K$ for multi-label classification and $\Omega = \Delta^{(K-1)}$ for multi-class classification. While TAILOR is proposed based on uniform priors $\mathbb{P}_0(\Omega) = \text{uniform}(\Omega)$, our analysis in this section holds for arbitrary \mathbb{P}_0 as long as the prior and posterior updates are modified accordingly in TAILOR.

First, we would like to mention a Bayesian regret upper bound for the contextual bandit formulation mentioned in 4.2. This provides one upper bound for TAILOR. As mentioned, the reduction to a contextual bandit is valid, but is only based on observing rewards and ignores the fact that TAILOR observes rewards and the full realizations $y^{t,j}$ of $\theta^{\alpha^{t,j}}$ that generate them. So one anticipates that this bound may be loose.

Proposition 5.1 (Russo & Van Roy (2014)). *Let π_{context} be the posterior sampling algorithm for linear contextual bandit presented in Russo & Van Roy (2014), the Bayesian regret is bounded by*

$$BR(\pi_{\text{context}}) \leq \tilde{O}(BM^{\frac{3}{4}}K^{\frac{3}{4}} \log T \sqrt{T})$$

where B is the batch size, M is the number of candidate algorithms, K is the number of classes, and T is the number of rounds.

We omit the proof in this paper and would like to point the readers to section 6.2.1 in Russo & Van Roy (2014) for the proof sketch. As mentioned in the paper, detailed confidence ellipsoid of least squares estimate and ellipsoid radius upper bound can be recovered from pages 14-15 of Abbasi-Yadkori et al. (2011).

We now present an upper bound on the Bayesian regret of TAILOR, which utilizes standard sub-Gaussian tail bounds based on observations of $y^{t,j}$ instead of confidence ellipsoids derived from only observing reward signals of $r^{t,j}$.

Theorem 5.2 (Proof in Appendix B). *The Bayesian regret of TAILOR is bounded by*

$$BR(\text{TAILOR}) \leq O(B\sqrt{MT(\log T + \log M)})$$

where B is the batch size, M is the number of candidate algorithms and T is total number of rounds.

We delay our complete proof to Appendix B. To highlight the key difference of our analysis from Russo & Van Roy (2014), their algorithm only rely on observations of $r^{t,j}$ for each round $t \in [T]$ and element $j \in [B]$ in a batch. To estimate $\theta^1, \dots, \theta^M$, they use the least squares estimator to form confidence ellipsoids. In our analysis, we utilize observations of $y \in H_t$ up to round t , where $H_t = \{\alpha^1, y^1, \alpha^2, y^2, \dots, \alpha^{t-1}, y^{t-1}\}$ denotes the history. We thus form confidence intervals directly around each of $\langle v^t, \theta^1 \rangle, \dots, \langle v^t, \theta^M \rangle$ by unbiased estimates $\{\langle v^t, y \rangle\}_{y \in H_t}$.

6. Experiments

In this section, we present results of TAILOR in terms of classification accuracy, class-balance of collected labels, and total number of positive examples for multi-label active search. Motivated by the observations, we also propose some future directions at the end.

6.1. Setup

Datasets. Our experiments span nine datasets with class-imbalance as shown in Table 1. For multi-label experiments, we experiment on four datasets including CelebA (Liu et al., 2018), COCO (Lin et al., 2014), VOC (Everingham et al., 2010) and Stanford Car (Krause et al., 2013) datasets. While the Stanford Car dataset is a multi-class classification dataset, we transform it into a multi-label dataset as detailed in Appendix A.2. For multi-class classification datasets, Kuzushiji-49 (Clanuwat et al., 2018) and Caltech256 (Griffin et al., 2007) are naturally unbalanced datasets, while CIFAR-10 with 2 classes, CIFAR-100 with 10 classes (Krizhevsky et al., 2009) and SVHN with 2 classes (Netzer et al., 2011) are derived from the original dataset following Zhang et al. (2022). Specifically, we keep the first $K - 1$ classes from the original dataset and treat the rest of the images as a large out-of-distribution K -th class.

Implementation Details. We conduct experiments on varying batch sizes anywhere from $B = 500$ to $B = 10000$. To mirror a limited training budget (Citovsky et al., 2021; Emam et al., 2021), we allow 10 or 20 batches in total for each dataset, making it extra challenging for our adaptive algorithm selection due to the limited rounds of interaction.

Moreover, we assumed observations of y are sampled from stationary distributions $\mathbb{P}_{\theta^1}, \dots, \mathbb{P}_{\theta^M}$ in our analysis. However, these distributions could be dynamically changing.

DATASET	K	N	CLASS IMB	BINARY IMB
CELEBA	40	162770	.0273	.2257
COCO	80	82081	.0028	.0367
VOC	20	10000	.0749	.0721
CAR	10	12948	.1572	.1200
KUZHISJI-49	49	23236	.0545	—
CALTECH256	256	24486	.0761	—
IMB CIFAR-10	2	50000	.1111	—
IMB CIFAR-100	10	50000	.0110	—
IMB SVHN	2	73257	.0724	—

Table 1. Details for multi-label and multi-class classification datasets. K and N denote the number of classes and pool size respectively. *Class Imb* represents the class imbalance ratio between the smallest and the largest class. We also report *Binary Imbalance Ratio* for multi-label datasets, which is defined as the average positive ratio over classes, i.e., $\frac{1}{K} \sum_{i \in [K]} (N_i / N)$ where N_i denotes the number of examples in class i .

In our implementation, we use a simple trick to discount the past observations, where we change the posterior update in Algorithm 2 to $a^i \leftarrow \gamma a^i + \sum_{j: \alpha^{t,j} = i} y^{t,j}$ and $b^i \leftarrow \gamma b^i + \sum_{j: \alpha^{t,j} = i} (1 - y^{t,j})$. We set the discounting factor γ to be .9 across all experiments. As will be discussed in Section 6.3, we find non-stationarity in $\{\mathbb{P}_{\theta^k}\}_{k=1}^M$ an interesting future direction to study. Lastly, we refer the readers to Appendix A for additional implementation details.

Baseline Algorithms. In our experiments, we choose a representative and popular subset of the deep AL algorithms discussed in Section 2 as our candidate algorithms. To demonstrate the ability of TAILOR, number of candidate algorithms M ranges from tens to hundreds for different datasets. The baselines can be divided into three categories:

- We include off-the-shelf AL algorithms such as **EMAL** (Wu et al., 2014) and **Weak Supervision** (Ranganathan et al., 2018) for multi-label classification and **Confidence sampling** (Settles, 2009), **BADGE** (Ash et al., 2019), **SIMILAR** (Kothawade et al., 2021) for multi-class classification. For all of the above algorithms, we transform them into iterative procedures as described in Appendix A.1. When implementing **SIMILAR**, instead of requiring access to a balanced holdout set, we construct the balanced set using training examples.
- We derive individual candidate algorithms based on a per-class decomposition (Boutell et al., 2004). For most likely positive sampling (Warmuth et al., 2001; 2003; Jiang et al., 2018), abbreviated as **MLP**, we obtain K algorithms where the i -th algorithm selects examples most likely to be in the i -th class. As detailed in Appendix A.5, we also include K individual **GALAXY** algorithms (Zhang et al., 2022) and K **Uncertainty sampling** algorithms for multi-label classification. As baseline for each type of algorithm, we simply interleave the

set of K algorithms uniformly at random.

- We compare against other adaptive meta selection algorithms, including **Random Meta** which chooses candidate algorithms uniform at random and **ALBL Sampling** (Hsu & Lin, 2015). The candidate algorithms include all of the baseline algorithms mentioned above.

6.2. Results

Multi-class and Multi-label Classification. For evaluation, we focus on TAILOR’s comparisons against both existing meta algorithms and the best baseline respectively. In all classification experiments, TAILOR uses the class diversity reward in Section 4.1. For accuracy metrics, we utilize mean average precision for multi-label classification and balanced accuracy for multi-class classification. As a class diversity metric, we look at the size of the smallest class based on collected labels. All of our experiments are measured based on active annotation performance over the pool (Zhang et al., 2022).

As shown in Figure 2 and Appendix D, when comparing against existing meta algorithms, TAILOR performs better on all datasets in terms of both accuracy and class diversity metrics. **ALBL sampling** performs similar to **Random Meta** in all datasets, suggesting the ineffectiveness of training accuracy based rewards proposed in Hsu & Lin (2015) and Pang et al. (2018). When comparing against the best baseline algorithm, TAILOR performs on par with the best baseline algorithm on eight out of nine datasets in terms of accuracy and on all datasets in terms of class diversity. On the CelebA dataset, TAILOR even outperforms the best baseline by significant margin in accuracy. As discussed in Appendix E, TAILOR achieves this by selecting a *combination* of other candidate algorithm instead of choosing only the best baseline. On four out of the nine datasets, TAILOR outperforms the best baseline in class diversity. Collectively, this shows the power of TAILOR in identifying the best candidate algorithms over different dataset scenarios. Shown in Appendix E, we also find TAILOR selects algorithms more aggressively than existing meta algorithms. The most frequent algorithms also align with the best baselines.

On the other hand, we also note both TAILOR and other meta algorithms tend to under-perform in the first few batches. We believe this is due to the necessary early exploration over all baseline algorithms. On the Caltech256 dataset, TAILOR under-performs **confidence sampling** in terms of accuracy, but collects a much more balanced dataset. If purely judged from an accuracy perspective, this shows a negative correlation between class diversity and accuracy and merits future research in designing alternative reward functions (see Section 6.3). Moreover, although **SIMILAR** and **Weak Supervision** under-perform in our settings, their inclusion in the experiments illustrates the resilience of

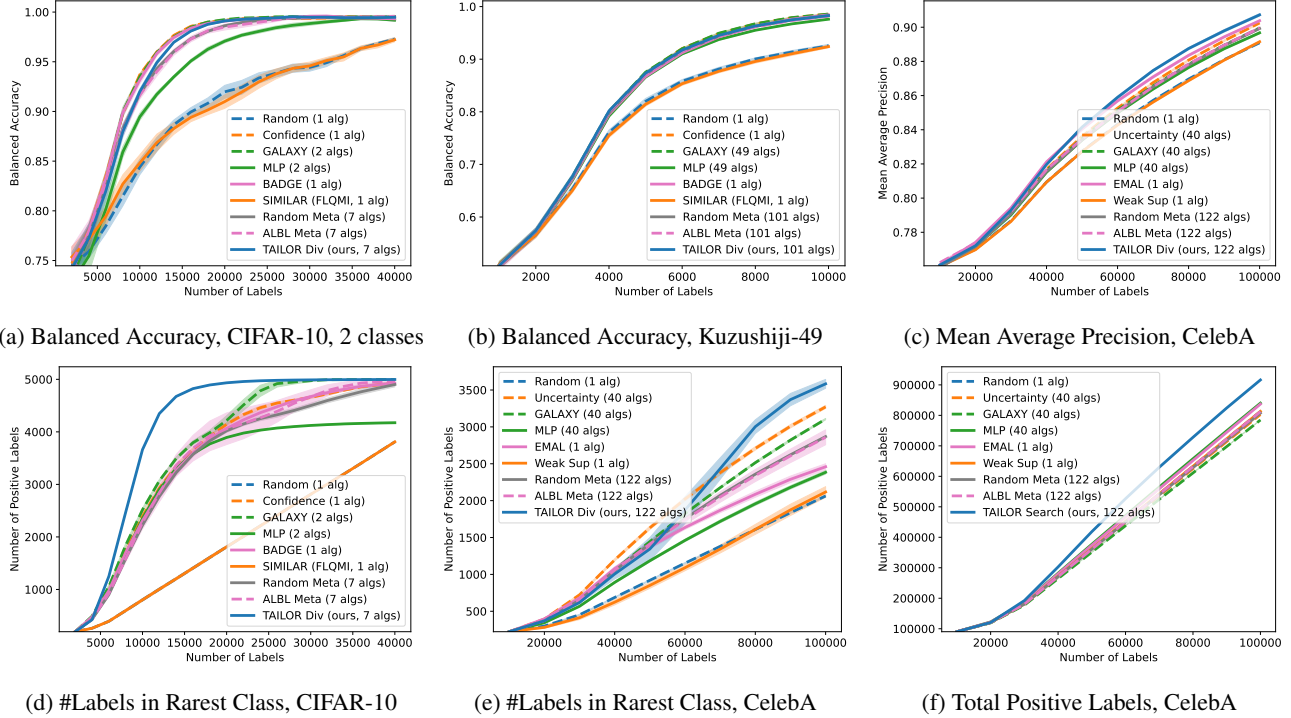


Figure 2. Performance of TAILOR against baselines on selected settings. First row shows accuracy metrics of the algorithms. (d) and (e) shows class-balancedness of labeled examples for multi-label and multi-class classifications. (f) shows the total number of positive labels collected for active search. All performances are averaged over four trials with standard error plotted for each algorithm. The curves are smoothed with a sliding window of size 3.

TAILOR (i.e., TAILOR performs well even if some of the algorithms included work relatively poorly). While **SIMILAR** usually performs well on unbalanced datasets, we attribute its under-performance to the lack of holdout set in our setting. As another practical failure scenario, we were unable to reproduce the results from [Ranganathan et al. \(2018\)](#) of the **Weak Supervision** algorithm.

Multi-label Search. We use the multi-label search reward proposed in Section 4.1. On three of the four datasets, TAILOR performs better than the best baseline algorithm in terms of total collected positive labels. On the fourth dataset, TAILOR performs second to and on par with the best baseline. This shows TAILOR’s ability in choosing the best candidate algorithms for multi-label active search.

6.3. Future Work

While our experiments focus on class-imbalanced settings, TAILOR’s effectiveness on balanced datasets warrants future study through further experiments and alternative reward design. In general, an interesting future direction involves designing better rewards functions that may incorporate accuracy or uncertainty measures. We also find studying non-stationarity in label distributions $\{\mathbb{P}_{\theta_i}\}_{i=1}^M$ an interesting next step.

7. Choosing Candidate Algorithms

Our paper proposes an adaptive selection procedure over candidate deep AL algorithms. When judging individual deep AL algorithms, current standards in the research community tend to focus on whether an algorithm performs well on *all* dataset and application instances. However, we see value in AL algorithms that perform well only in certain instances. Consider, for example, an AL algorithm that performs well on 25% of previous applications, but poorly on the other 75%. One may wish to include this algorithm in TAILOR because the new application might be similar to those where it performs well. From the perspective of TAILOR, a “good” AL algorithm need not perform well on all or even most of a range of datasets, it just needs to perform well on a significant fraction of datasets.

On the other hand, as suggested by our regret bound that scales with M , one should not include too many algorithms. In fact, there are exponential number of possible AL algorithms, which could easily surpass our labeling budget and overwhelm the meta selection algorithm. In practice, one could leverage extra information such as labeling budget, batch size and model architecture to choose proper set of candidate algorithms to target their settings.

Acknowledgement

We would like to thank Aude Hofleitner and Shawndra Hill for the support of this research project, and Kevin Jamieson, Yifang Chen and Andrew Wagenmaker for insightful discussions. Robert Nowak would like to thank the support of NSF Award 2112471.

References

Abbasi-Yadkori, Y., Pál, D., and Szepesvári, C. Improved algorithms for linear stochastic bandits. *Advances in neural information processing systems*, 24, 2011.

Aggarwal, U., Popescu, A., and Hudelot, C. Active learning for imbalanced datasets. In *Proceedings of the IEEE/CVF Winter Conference on Applications of Computer Vision*, pp. 1428–1437, 2020.

Ash, J., Goel, S., Krishnamurthy, A., and Kakade, S. Gone fishing: Neural active learning with fisher embeddings. *Advances in Neural Information Processing Systems*, 34: 8927–8939, 2021.

Ash, J. T., Zhang, C., Krishnamurthy, A., Langford, J., and Agarwal, A. Deep batch active learning by diverse, uncertain gradient lower bounds. *arXiv preprint arXiv:1906.03671*, 2019.

Balcan, M.-F., Beygelzimer, A., and Langford, J. Agnostic active learning. In *Proceedings of the 23rd international conference on Machine learning*, pp. 65–72, 2006.

Baram, Y., Yaniv, R. E., and Luz, K. Online choice of active learning algorithms. *Journal of Machine Learning Research*, 5(Mar):255–291, 2004.

Beck, N., Sivasubramanian, D., Dani, A., Ramakrishnan, G., and Iyer, R. Effective evaluation of deep active learning on image classification tasks. *arXiv preprint arXiv:2106.15324*, 2021.

Beluch, W. H., Genewein, T., Nürnberger, A., and Köhler, J. M. The power of ensembles for active learning in image classification. In *Proceedings of the IEEE conference on computer vision and pattern recognition*, pp. 9368–9377, 2018.

Boutell, M. R., Luo, J., Shen, X., and Brown, C. M. Learning multi-label scene classification. *Pattern recognition*, 37(9):1757–1771, 2004.

Cai, X. Active learning for imbalanced data: The difficulty and proportions of class matter. *Wireless Communications and Mobile Computing*, 2022, 2022.

Citovsky, G., DeSalvo, G., Gentile, C., Karydas, L., Rajagopalan, A., Rostamizadeh, A., and Kumar, S. Batch active learning at scale. *Advances in Neural Information Processing Systems*, 34:11933–11944, 2021.

Clanuwat, T., Bober-Irizar, M., Kitamoto, A., Lamb, A., Yamamoto, K., and Ha, D. Deep learning for classical japanese literature. *arXiv preprint arXiv:1812.01718*, 2018.

Coleman, C., Chou, E., Katz-Samuels, J., Culatana, S., Bailis, P., Berg, A. C., Nowak, R., Sumbaly, R., Zaharia, M., and Yalniz, I. Z. Similarity search for efficient active learning and search of rare concepts. In *Proceedings of the AAAI Conference on Artificial Intelligence*, volume 36, pp. 6402–6410, 2022.

Donmez, P., Carbonell, J. G., and Bennett, P. N. Dual strategy active learning. In *European Conference on Machine Learning*, pp. 116–127. Springer, 2007.

Ducoffe, M. and Precioso, F. Adversarial active learning for deep networks: a margin based approach. *arXiv preprint arXiv:1802.09841*, 2018.

Elenter, J., NaderiAlizadeh, N., and Ribeiro, A. A lagrangian duality approach to active learning. *arXiv preprint arXiv:2202.04108*, 2022.

Emam, Z. A. S., Chu, H.-M., Chiang, P.-Y., Czaja, W., Leipman, R., Goldblum, M., and Goldstein, T. Active learning at the imagenet scale. *arXiv preprint arXiv:2111.12880*, 2021.

Everingham, M., Van Gool, L., Williams, C. K., Winn, J., and Zisserman, A. The pascal visual object classes (voc) challenge. *International journal of computer vision*, 88(2):303–338, 2010.

Gal, Y., Islam, R., and Ghahramani, Z. Deep bayesian active learning with image data. In *International Conference on Machine Learning*, pp. 1183–1192. PMLR, 2017.

Geifman, Y. and El-Yaniv, R. Deep active learning over the long tail. *arXiv preprint arXiv:1711.00941*, 2017.

Gissin, D. and Shalev-Shwartz, S. Discriminative active learning. *arXiv preprint arXiv:1907.06347*, 2019.

Gonsior, J., Thiele, M., and Lehner, W. Imital: Learning active learning strategies from synthetic data. *arXiv preprint arXiv:2108.07670*, 2021.

Griffin, G., Holub, A., and Perona, P. Caltech-256 object category dataset. 2007.

He, K., Zhang, X., Ren, S., and Sun, J. Deep residual learning for image recognition. In *Proceedings of the IEEE conference on computer vision and pattern recognition*, pp. 770–778, 2016.

Hsu, W.-N. and Lin, H.-T. Active learning by learning. In *Twenty-Ninth AAAI conference on artificial intelligence*, 2015.

Jiang, S., Malkomes, G., Abbott, M., Moseley, B., and Garnett, R. Efficient nonmyopic batch active search. In *32nd Conference on Neural Information Processing Systems (NeurIPS 2018)*, 2018.

Jin, Q., Yuan, M., Wang, H., Wang, M., and Song, Z. Deep active learning models for imbalanced image classification. *Knowledge-Based Systems*, 257:109817, 2022.

Kingma, D. P. and Ba, J. Adam: A method for stochastic optimization. *arXiv preprint arXiv:1412.6980*, 2014.

Konyushkova, K., Sznitman, R., and Fua, P. Learning active learning from data. *Advances in neural information processing systems*, 30, 2017.

Kothawade, S., Beck, N., Killamsetty, K., and Iyer, R. Similar: Submodular information measures based active learning in realistic scenarios. *Advances in Neural Information Processing Systems*, 34:18685–18697, 2021.

Krause, J., Stark, M., Deng, J., and Fei-Fei, L. 3d object representations for fine-grained categorization. In *Proceedings of the IEEE international conference on computer vision workshops*, pp. 554–561, 2013.

Kremer, J., Steenstrup Pedersen, K., and Igel, C. Active learning with support vector machines. *Wiley Interdisciplinary Reviews: Data Mining and Knowledge Discovery*, 4(4):313–326, 2014.

Krizhevsky, A., Hinton, G., et al. Learning multiple layers of features from tiny images. 2009.

Lattimore, T. and Szepesvári, C. *Bandit algorithms*. Cambridge University Press, 2020.

Lin, T.-Y., Maire, M., Belongie, S., Hays, J., Perona, P., Ramanan, D., Dollár, P., and Zitnick, C. L. Microsoft coco: Common objects in context. In *European conference on computer vision*, pp. 740–755. Springer, 2014.

Liu, Z., Luo, P., Wang, X., and Tang, X. Large-scale celeb-faces attributes (celeba) dataset. *Retrieved August, 15 (2018):11*, 2018.

Löffler, C. and Mutschler, C. Iale: Imitating active learner ensembles. *Journal of Machine Learning Research*, 23 (107):1–29, 2022.

Min, X.-Y., Qian, K., Zhang, B.-W., Song, G., and Min, F. Multi-label active learning through serial-parallel neural networks. *Knowledge-Based Systems*, 251:109226, 2022.

Mohamadi, M. A., Bae, W., and Sutherland, D. J. Making look-ahead active learning strategies feasible with neural tangent kernels. *arXiv preprint arXiv:2206.12569*, 2022.

Netzer, Y., Wang, T., Coates, A., Bissacco, A., Wu, B., and Ng, A. Y. Reading digits in natural images with unsupervised feature learning. 2011.

Pang, K., Dong, M., Wu, Y., and Hospedales, T. M. Dynamic ensemble active learning: A non-stationary bandit with expert advice. In *2018 24th International Conference on Pattern Recognition (ICPR)*, pp. 2269–2276. IEEE, 2018.

Ranganathan, H., Venkateswara, H., Chakraborty, S., and Panchanathan, S. Multi-label deep active learning with label correlation. In *2018 25th IEEE International Conference on Image Processing (ICIP)*, pp. 3418–3422. IEEE, 2018.

Russo, D. and Van Roy, B. Learning to optimize via posterior sampling. *Mathematics of Operations Research*, 39 (4):1221–1243, 2014.

Sener, O. and Savarese, S. Active learning for convolutional neural networks: A core-set approach. *arXiv preprint arXiv:1708.00489*, 2017.

Settles, B. Active learning literature survey. 2009.

Shao, J., Wang, Q., and Liu, F. Learning to sample: an active learning framework. In *2019 IEEE International Conference on Data Mining (ICDM)*, pp. 538–547. IEEE, 2019.

Thompson, W. R. On the likelihood that one unknown probability exceeds another in view of the evidence of two samples. *Biometrika*, 25(3-4):285–294, 1933.

Tong, S. and Koller, D. Support vector machine active learning with applications to text classification. *Journal of machine learning research*, 2(Nov):45–66, 2001.

Wang, H., Huang, W., Margenot, A., Tong, H., and He, J. Deep active learning by leveraging training dynamics. *arXiv preprint arXiv:2110.08611*, 2021.

Warmuth, M. K., Rätsch, G., Mathieson, M., Liao, J., and Lemmen, C. Active learning in the drug discovery process. In *NIPS*, pp. 1449–1456, 2001.

Warmuth, M. K., Liao, J., Rätsch, G., Mathieson, M., Putta, S., and Lemmen, C. Active learning with support vector machines in the drug discovery process. *Journal of chemical information and computer sciences*, 43(2):667–673, 2003.

Wu, J., Sheng, V. S., Zhang, J., Zhao, P., and Cui, Z. Multi-label active learning for image classification. In *2014 IEEE international conference on image processing (ICIP)*, pp. 5227–5231. IEEE, 2014.

Wu, J., Sheng, V. S., Zhang, J., Li, H., Dadakova, T., Swisher, C. L., Cui, Z., and Zhao, P. Multi-label active learning algorithms for image classification: Overview and future promise. *ACM Computing Surveys (CSUR)*, 53(2):1–35, 2020.

Zhan, X., Wang, Q., Huang, K.-h., Xiong, H., Dou, D., and Chan, A. B. A comparative survey of deep active learning. *arXiv preprint arXiv:2203.13450*, 2022.

Zhang, J., Jain, L., and Jamieson, K. Learning to actively learn: A robust approach. *arXiv preprint arXiv:2010.15382*, 2020.

Zhang, J., Katz-Samuels, J., and Nowak, R. Galaxy: Graph-based active learning at the extreme. *arXiv preprint arXiv:2202.01402*, 2022.

A. Implementation Details

A.1. Deep Active Learning Decomposition

For any uncertainty sampling algorithm, picking the top- B most uncertain examples can be easily decomposed into an iterative procedure that picks the next most uncertain example. Next, for diversity based deep active learning algorithms, one usually rely on an greedy iterative procedure to collect a batch, e.g. K-means++ for BADGE (Ash et al., 2019), greedy K-centers for Coreset (Sener & Savarese, 2017) and greedy submodular optimization for SIMILAR (Kothawade et al., 2021). Lastly, deep active learning algorithms such as Cluster-Margin (Citovsky et al., 2021) and GALAXY (Zhang et al., 2022) have already proposed their algorithms as iterative procedures that select unlabeled examples sequentially.

A.2. Stanford Car Multi-label Dataset

We transform the original labels into 10 binary classes of

1. If the brand is “Audi”.
2. If the brand is “BMW”.
3. If the brand is “Chevrolet”.
4. If the brand is “Dodge”.
5. If the brand is “Ford”.
6. If the car type is “Convertible”.
7. If the car type is “Coupe”.
8. If the car type is “SUV”.
9. If the car type is “Van”.
10. If the car is made in or before 2009.

A.3. Negative Weighting for Common Classes

For multi-label classifications, for some classes, there could be more positive associations (label of 1s) than negative associations (label of 0s). Therefore, in those classes, the rarer labels are negative. In class diverse reward $\langle v_{div}^t, y \rangle$ in Section 4.1, we implement an additional weighting of $\mathbb{1}_{rare}^t * v_{div}^t$, where $*$ denotes an elementwise multiplication. Here, each element $\mathbb{1}_{rare,i}^t \in \{1, -1\}$ takes value -1 when $\text{COUNT}^t(i)$ is larger than half the size of labeled set. This negative weighting can be seen as upsampling negative class associations when positive associations are the majority.

A.4. Model Training

All of our experiments are conducted using the ResNet-18 architecture (He et al., 2016) pretrained on ImageNet. We use the Adam optimizer (Kingma & Ba, 2014) with learning rate of 1e-4 and weight decay of 5e-5.

A.5. Baseline Algorithms

In the original GALAXY work by (Zhang et al., 2022), their algorithm construct K one-vs-rest linear graphs, one for each class. GALAXY requires finding the shortest shortest path among all K graphs, an operation whose computation scales linearly in K . When K is large, this becomes computationally prohibitive to run. Therefore, we instead include K separate GALAXY algorithms, each only bisecting on one of the one-vs-rest graphs. This is equivalent with running K GALAXY algorithms, one for each binary classification task between class $i \in [K]$ and the rest. As a baseline, we interleave these algorithms uniformly at random.

For Uncertainty sampling in multi-label settings, we simply have K individual uncertainty sampling algorithms, where the i -th algorithm samples the most uncertain example based only on the binary classification task of class i .

B. Proof of Theorem 5.2

Our proof follows a similar procedure from regret analysis for Thompson Sampling of the stochastic multi-armed bandit problem (Lattimore & Szepesvári, 2020). Let $\alpha^t := \{\alpha^{t,j}\}_{j=1}^B$ and $y^t := \{y^{t,j}\}_{j=1}^B$ denote the actions and observations from the i -th round. We define the history up to t as $H_t = \{\alpha^1, y^1, \alpha^2, y^2, \dots, \alpha^{t-1}, y^{t-1}\}$. Moreover, for each $i \in [M]$, we define $H_{t,i} = \{y^{t',j} \in H_t : \alpha^{t',j} = i\}$ as the history of all observations made by choosing the i -th arm (algorithm).

Now we analyze reward estimates at each round t . When given history H_t and arm $i \in [M]$, each observation $y \in H_{t,i}$ is an unbiased estimate of θ^i as $y \sim \mathbb{P}_{\theta^i}$. Therefore, for any fixed v^t , $\langle v^t, y \rangle$ is an unbiased estimate of the expected reward $\langle v^t, \theta^i \rangle$, which we denote by $\mu^{t,i}$.

For each arm i , we can then obtain empirical reward estimate $\bar{\mu}^{t,i}$ of the true expected reward $\mu^{t,i}$ by $\bar{\mu}^{t,i} := \frac{1}{1 \vee |H_{t,i}|} \sum_{y \in H_{t,i}} \langle v^t, y \rangle$ where $\bar{\mu}^{t,i} = 0$ if $|H_{t,i}| = 0$. Since expected rewards and reward estimates are bounded by $[-1, 1]$, by standard sub-Gaussian tail bounds, we can then construct confidence interval,

$$\mathbb{P}(\forall i \in [M], t \in [T], |\bar{\mu}^{t,i} - \mu^{t,i}| \leq d^{t,i}) \geq 1 - \frac{1}{T}$$

where $d^{t,i} := \sqrt{\frac{8 \log(MT^2)}{1 \vee |H_{t,i}|}}$. Additionally, we define upper confidence bound as $U^{t,i} = \text{clip}_{[-1,1]}(\bar{\mu}^{t,i} + d^{t,i})$.

At each iteration t , we have the posterior distribution $\mathbb{P}(\Theta = \cdot | H_t)$ of the ground truth $\Theta = \{\theta^i\}_{i=1}^M$. $\widehat{\Theta} = \{\widehat{\theta}^i\}_{i=1}^M$ is sampled from this posterior. Consider $i_*^t = \arg \max_{i \in M} \langle v^t, \theta^i \rangle$ and $\alpha^{t,j} = \arg \max_{i \in M} \langle v^t, \widehat{\theta}^i \rangle$. The distribution of i_*^t is determined by the posterior $\mathbb{P}(\Theta = \cdot | H_t)$. The distribution of $\alpha^{t,j}$ is determined by the distribution of $\widehat{\Theta}$, which is also $\mathbb{P}(\Theta = \cdot | H_t)$. Therefore, i_*^t and $\alpha^{t,j}$ are identically distributed. Furthermore, since the upper confidence bounds are deterministic functions of i when given H_t , we then have $\mathbb{E}[U^{t,\alpha^{t,j}} | H_t] = \mathbb{E}[U^{t,i_*^t} | H_t]$.

As a result, we upper bound the Bayesian regret by

$$\begin{aligned} BR(\text{TAILOR}) &= \mathbb{E} \left[\sum_{t=1}^T \sum_{j=1}^B \mu^{t,i_*^t} - \mu^{t,\alpha^{t,j}} \right] \\ &= \mathbb{E} \left[\sum_{t=1}^T \sum_{j=1}^B (\mu^{t,i_*^t} - U^{t,i_*^t}) + (U^{t,\alpha^{t,j}} - \mu^{t,\alpha^{t,j}}) \right]. \end{aligned}$$

Now, note that since $\bar{\mu}^{t,i} \in [-1, 1]$ we have $\text{clip}_{[-1,1]}(\bar{\mu}^{t,i} + d^{t,i}) = \text{clip}_{[-\infty,1]}(\bar{\mu}^{t,i} + d^{t,i})$, where only the upper clip takes effect. Based on the sub-Gaussian confidence intervals $\mathbb{P}(\forall i \in [M], t \in [T], |\bar{\mu}^{t,i} - \mu^{t,i}| \leq d^{t,i}) \geq 1 - \frac{1}{T}$, we can derive the following two confidence bounds:

$$\begin{aligned} \mathbb{P}(\forall i \in [M], t \in [T], \mu^{t,i} > U^{t,i}) &= \mathbb{P}(\forall i \in [M], t \in [T], \mu^{t,i} > \text{clip}_{[-1,1]}(\bar{\mu}^{t,i} + d^{t,i})) \\ &= \mathbb{P}(\forall i \in [M], t \in [T], \mu^{t,i} > \bar{\mu}^{t,i} + d^{t,i}), \text{ since } \mu^{t,i} \leq 1 \\ &= \mathbb{P}(\forall i \in [M], t \in [T], \mu^{t,i} - \bar{\mu}^{t,i} > d^{t,i}) \leq \frac{1}{2T} \\ \mathbb{P}(\forall i \in [M], t \in [T], U^{t,i} - \mu^{t,i} > 2d^{t,i}) &= \mathbb{P}(\forall i \in [M], t \in [T], \text{clip}_{[-1,1]}(\bar{\mu}^{t,i} + d^{t,i}) - \mu^{t,i} > 2d^{t,i}) \\ &\leq \mathbb{P}(\forall i \in [M], t \in [T], \bar{\mu}^{t,i} + d^{t,i} - \mu^{t,i} > 2d^{t,i}) \\ &= \mathbb{P}(\forall i \in [M], t \in [T], \bar{\mu}^{t,i} - \mu^{t,i} > d^{t,i}) \leq \frac{1}{2T}. \end{aligned}$$

Now with the decomposition,

$$\begin{aligned} BR(\text{TAILOR}) &= \mathbb{E} \left[\sum_{t=1}^T \sum_{j=1}^B \mu^{t,i_*^t} - \mu^{t,\alpha^{t,j}} \right] \\ &= \mathbb{E} \left[\sum_{t=1}^T \sum_{j=1}^B \mu^{t,i_*^t} - U^{t,i_*^t} \right] + \mathbb{E} \left[\sum_{t=1}^T \sum_{j=1}^B U^{t,\alpha^{t,j}} - \mu^{t,\alpha^{t,j}} \right] \end{aligned}$$

we can bound the two expectations individually.

First, to bound $\mathbb{E} \left[\sum_{t=1}^T \sum_{j=1}^B \mu^{t,i_*^t} - U^{t,i_*^t} \right]$, we note that $\mu^{t,i_*^t} - U^{t,i_*^t}$ is negative with high probability. Also, the maximum value this can take is bounded by 2 as $\mu^{t,i}, U^{t,i} \in [-1, 1]$. Therefore, we have

$$\mathbb{E} \left[\sum_{t=1}^T \sum_{j=1}^B \mu^{t,i_*^t} - U^{t,i_*^t} \right] \leq \left(\sum_{t=1}^T \sum_{j=1}^B 0 \cdot \mathbb{P}(\mu^{t,i_*^t} \leq U^{t,i_*^t}) + 2 \cdot \mathbb{P}(\mu^{t,i_*^t} > U^{t,i_*^t}) \right) \leq 2TB \cdot \frac{1}{2T} = B.$$

Next, to bound $\mathbb{E} \left[\sum_{t=1}^T \sum_{j=1}^B U^{t,\alpha^{t,j}} - \mu^{t,\alpha^{t,j}} \right]$ we decompose it similar to the above:

$$\begin{aligned} \mathbb{E} \left[\sum_{t=1}^T \sum_{j=1}^B U^{t,\alpha^{t,j}} - \mu^{t,\alpha^{t,j}} \right] &\leq \left(\sum_{t=1}^T \sum_{j=1}^B 2\mathbb{P}(U^{t,\alpha^{t,j}} - \mu^{t,\alpha^{t,j}} > 2d^{t,i}) \right) + \left(\sum_{t=1}^T \sum_{j=1}^B 2d^{t,i} \right) \\ &\leq B + \left(\sum_{t=1}^T \sum_{j=1}^B \sqrt{\frac{32 \log(MT^2)}{1 \vee |H_{t,\alpha^{t,j}}|}} \right) \end{aligned}$$

where recall that $|H_{t,i}|$ is the number of samples collected using algorithm i in rounds $\leq t$.

To bound the summation, we utilize the fact that $\frac{1}{1 \vee |H_{t,i}|} \leq \frac{B}{k}$ for each $k \in [|H_{t,i}|, |H_{t+1,i}|]$, since $|H_{t+1,i}| - |H_{t,i}| \leq B$. As a result, we get

$$\begin{aligned} &\sum_{t=1}^T \sum_{j=1}^B \sqrt{\frac{32 \log(MT^2)}{1 \vee |H_{t,\alpha^{t,j}}|}} \\ &\leq \sum_{t=1}^T \sum_{i=1}^M \sum_{k=1}^{|H_{t,i}|} \sqrt{\frac{32 \log(MT^2) \cdot B}{k}} \\ &\leq O(\sqrt{B(\log T + \log M)} \sum_{i=1}^M \sqrt{|H_{t,i}|}) \\ &\leq O(\sqrt{B(\log T + \log M)}) \cdot O(\sqrt{BMT}) = O(B\sqrt{MT(\log T + \log M)}) \end{aligned}$$

where last two inequalities follow from simple algebra and the fact that $\sum_{i=1}^M |H_{t,i}| = TB$.

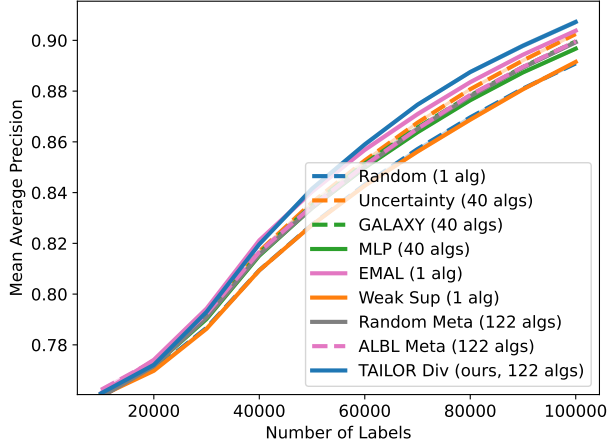
Finally, to combine all of the bounds above, we get $BR(\text{TAILOR}) \leq B + B + O(B\sqrt{MT(\log T + \log M)}) = O(B\sqrt{MT(\log T + \log M)})$.

C. Time Complexity

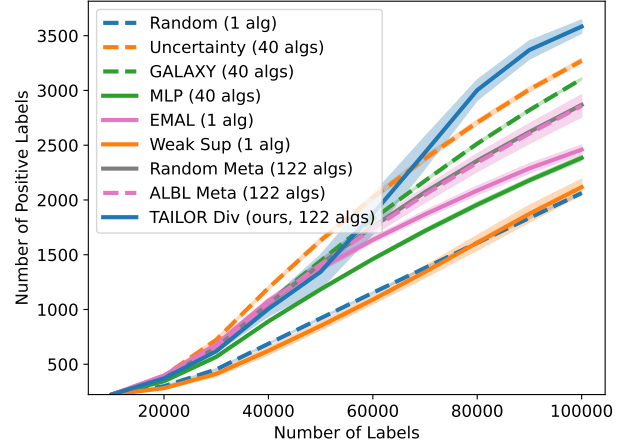
Let N_{train} denote the total neural network training. The time complexity of collecting each batch for each active learning algorithm \mathcal{A}_i can be separated into P_i and Q_i , which are the computation complexity for preprocessing and selection of each example respectively. As examples of preprocessing, BADGE (Ash et al., 2019) computes gradient embeddings, SIMILAR (Kothawade et al., 2021) further also compute similarity kernels, GALAXY (Zhang et al., 2022) constructs linear graphs, etc. The selection complexities are the complexities of each iteration of K-means++ in BADGE, greedy submodular optimization in SIMILAR, and shortest shortest path computation in GALAXY. Therefore, for any individual algorithm \mathcal{A}_i , the computation complexity is then $O(N_{train} + TP_i + TBQ_i)$ where T is the total number of rounds and B is the batch size. When running TAILOR, as we do not know which algorithms are selected, we provide a worst case upper bound of $O(N_{train} + T \cdot (\sum_{i=1}^M P_i) + TB \cdot \max_{i \in [M]} Q_i)$, where the preprocessing is done for every candidate algorithm. In practice, some of the preprocessing operations such as gradient embedding computation could be shared among multiple algorithms, thus only need to be computed once. While the computation of rewards and Thompson sampling updates incur some extra complexity, they are usually dominated in practice by the complexity of neural network training and running each candidate algorithm.

D. Full Results

D.1. Multi-label Classification

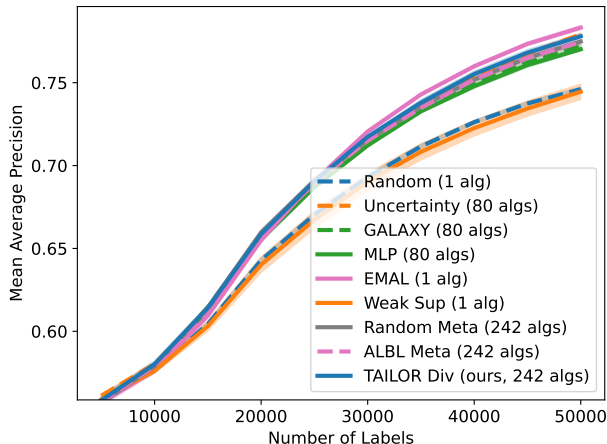


(a) Mean Average Precision

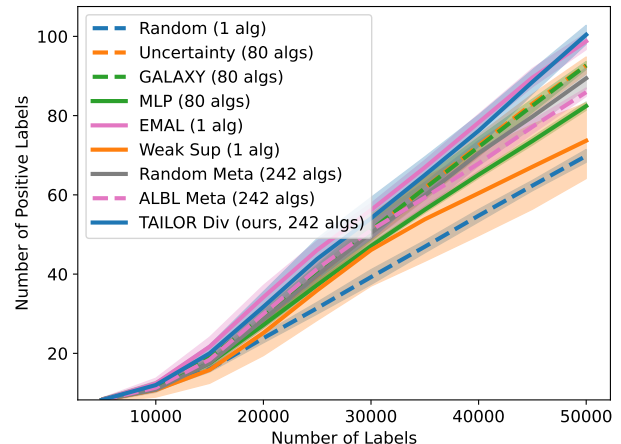


(b) Number of Labels in Rarest Class

Figure 3. CelebA

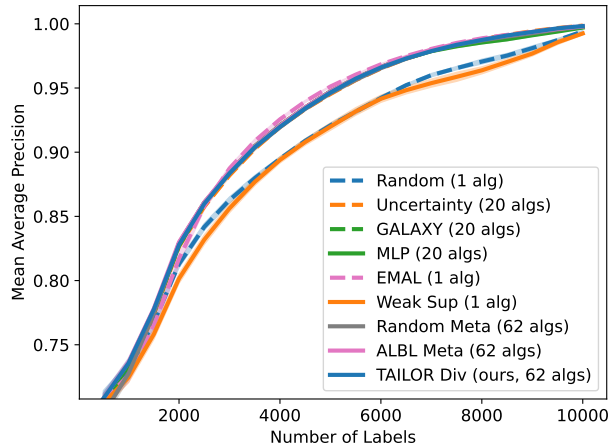


(a) Mean Average Precision

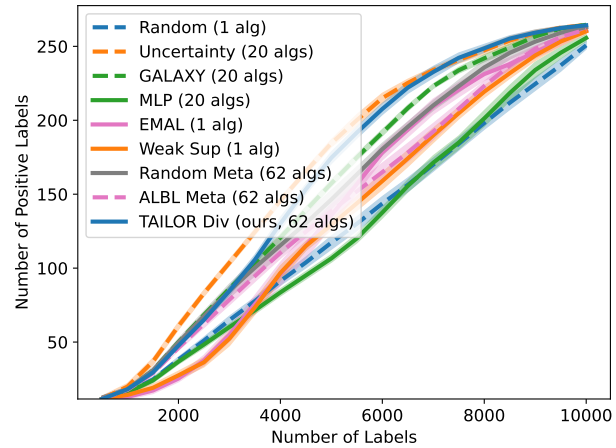


(b) Number of Labels in Rarest Class

Figure 4. COCO

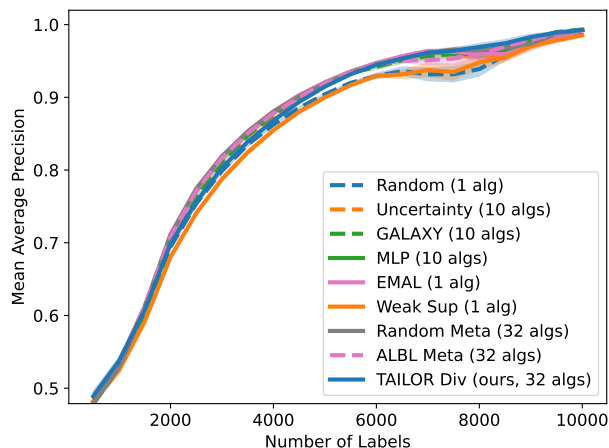


(a) Mean Average Precision

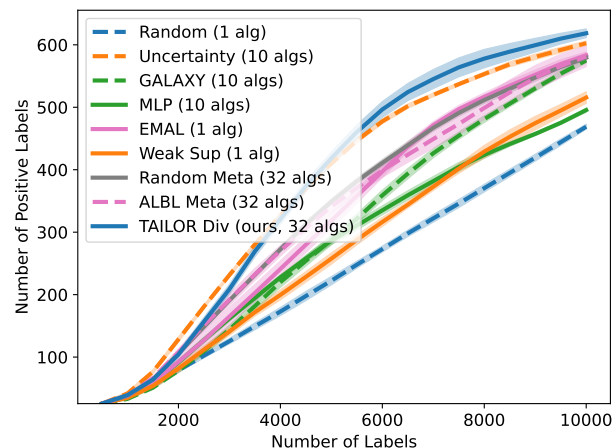


(b) Number of Labels in Rarest Class

Figure 5. VOC



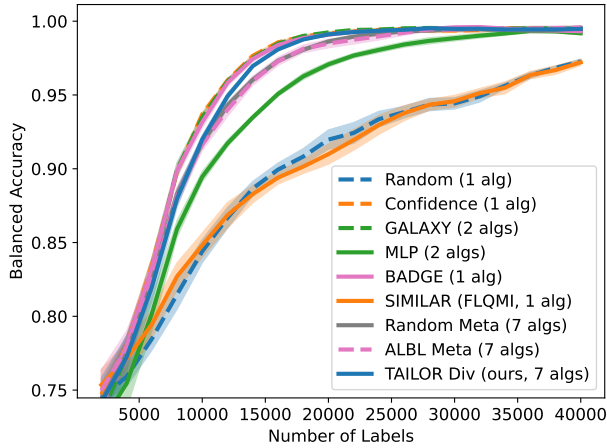
(a) Mean Average Precision



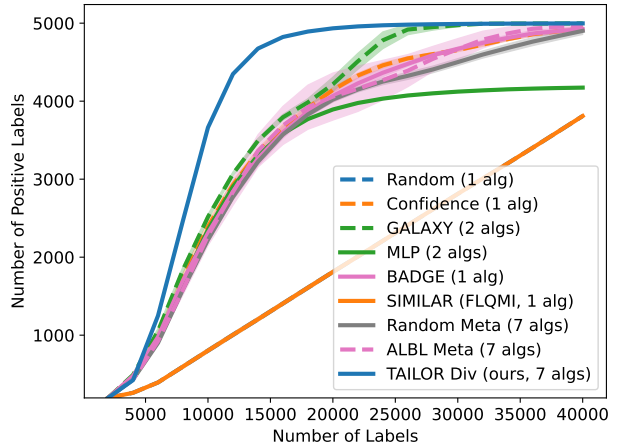
(b) Number of Labels in Rarest Class

Figure 6. Stanford Car

D.2. Multi-class Classification

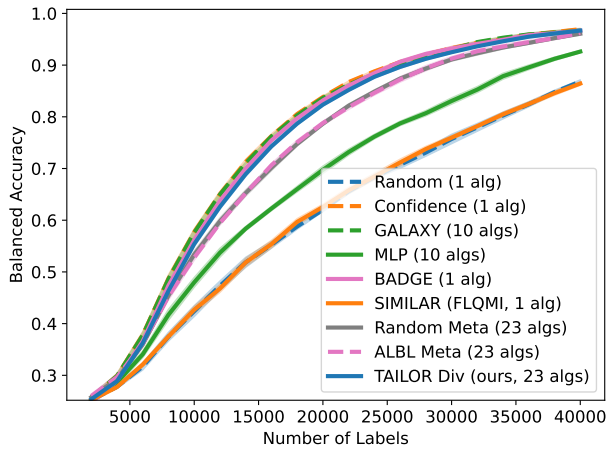


(a) Balanced Accuracy

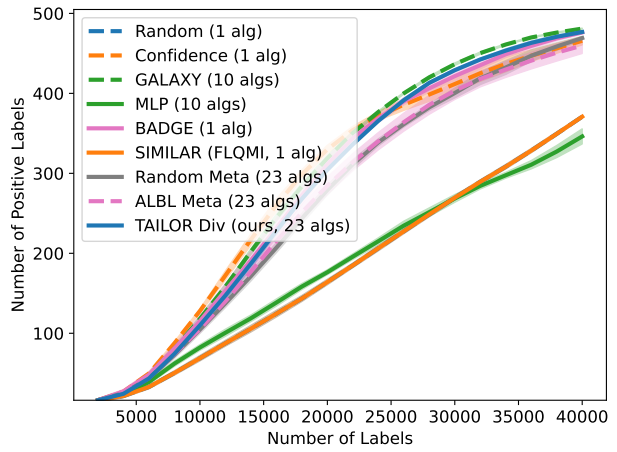


(b) Number of Labels in Rarest Class

Figure 7. CIFAR-10, 2 classes



(a) Balanced Accuracy



(b) Number of Labels in Rarest Class

Figure 8. CIFAR-100, 10 classes

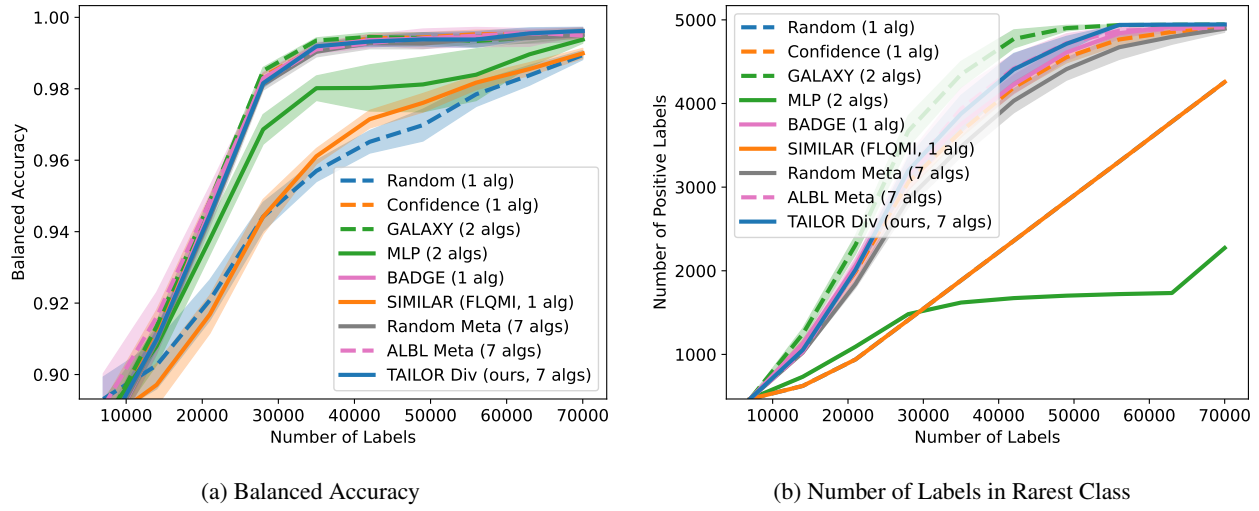


Figure 9. SVHN, 2 classes

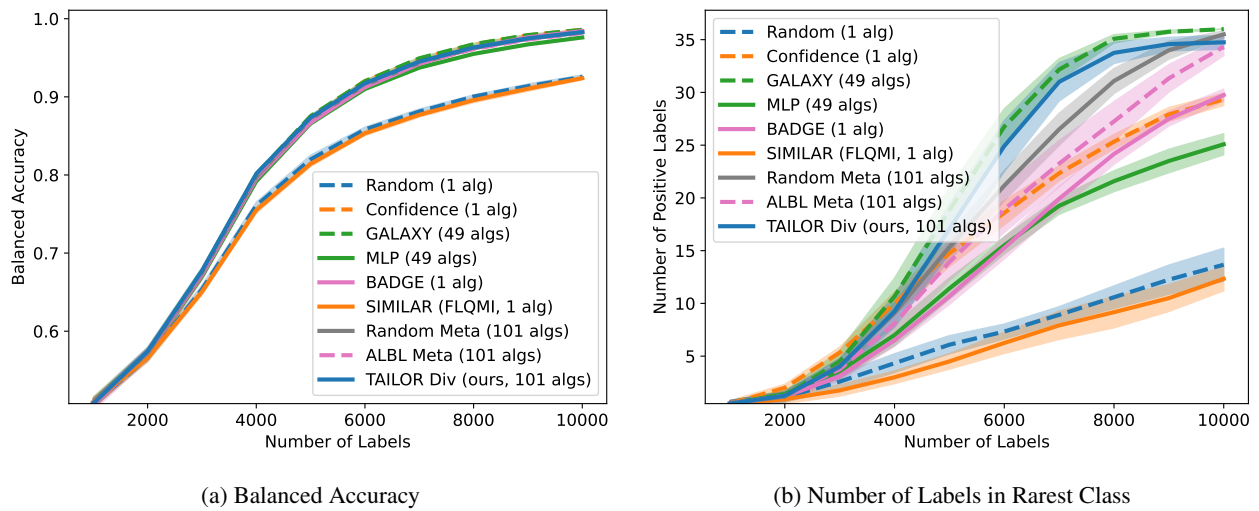
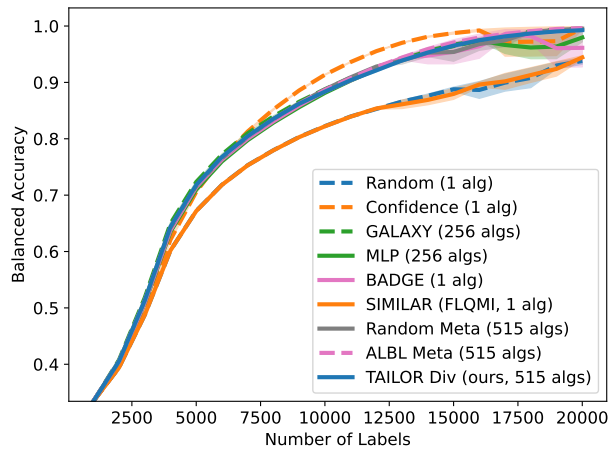
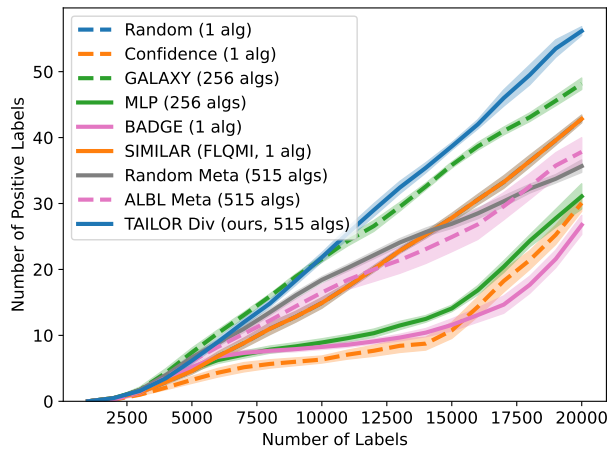


Figure 10. Kuzushiji-49



(a) Balanced Accuracy



(b) Number of Labels in Rarest Class

Figure 11. Caltech256

D.3. Multi-label Search

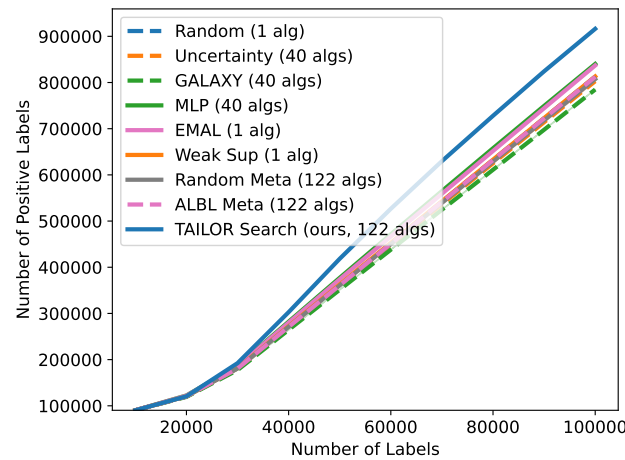


Figure 12. CelebA, Total Number of Positive Labels

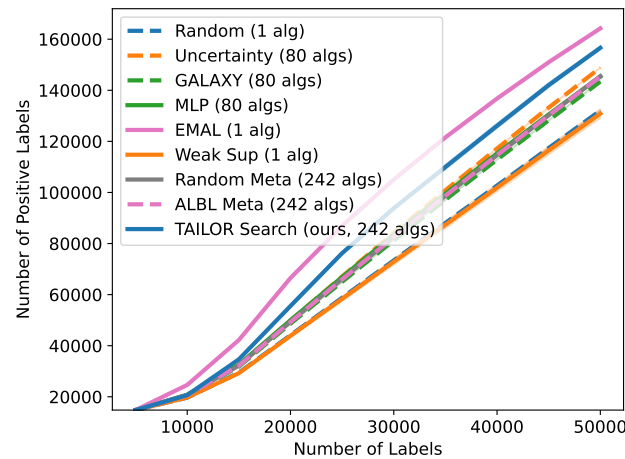


Figure 13. COCO, Total Number of Positive Labels

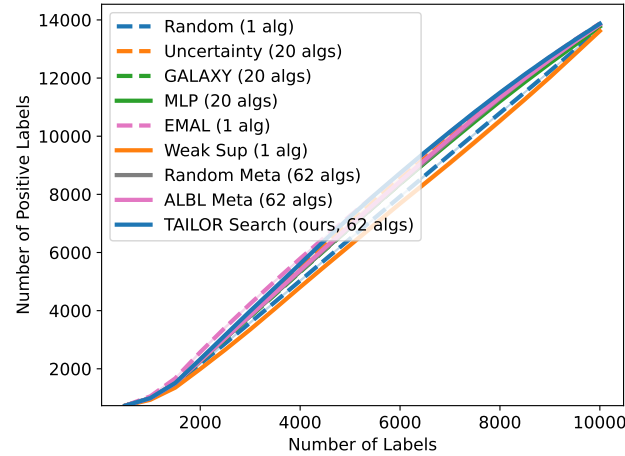


Figure 14. VOC, Total Number of Positive Labels

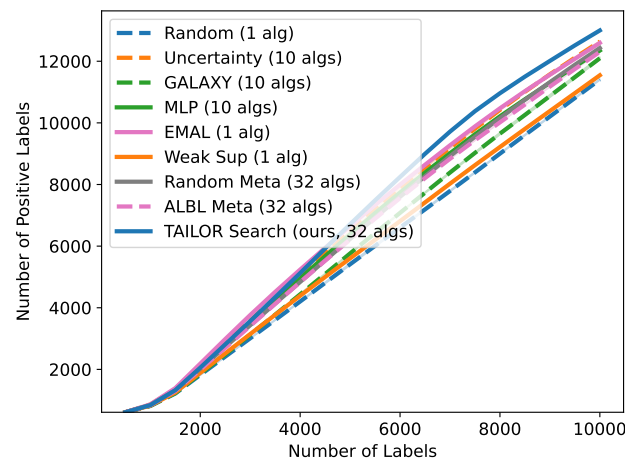


Figure 15. Stanford Car, Total Number of Positive Labels

E. What Algorithms Does TAILOR Choose?

In the following two figures, we can see TAILOR chooses a non-uniform set of algorithms to focus on for each dataset. On CelebA, TAILOR out-perform the best baseline, EMAL sampling, by a significant margin. As we can see, TAILOR rely on selecting a *combination* of other candidate algorithms instead of only selecting EMAL.

On the other hand, for the Stanford car dataset, we see TAILOR 's selection mostly align with the baselines that perform well especially in the later phase.

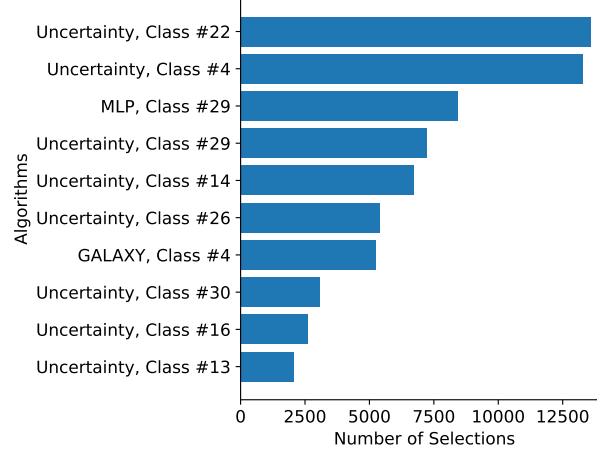


Figure 16. TAILOR Top-10 Most Selected Candidate Algorithms on CelebA Dataset

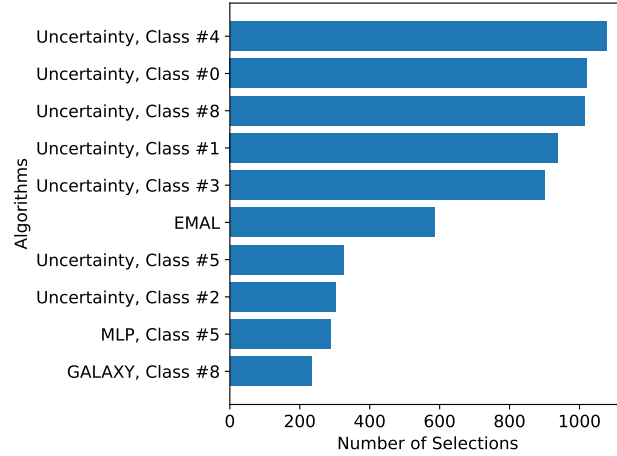


Figure 17. TAILOR Top-10 Most Selected Candidate Algorithms on Stanford Car Dataset

In the following figures, we plot the number of times the most frequent candidate algorithm is chosen. As can be shown, TAILOR chooses candidate algorithm much more aggressively than other meta algorithms in seven out of the nine settings. In the other two settings, unbalanced CIFAR-100 and SVHN, TAILOR is still comparatively aggressive as ALBL sampling.

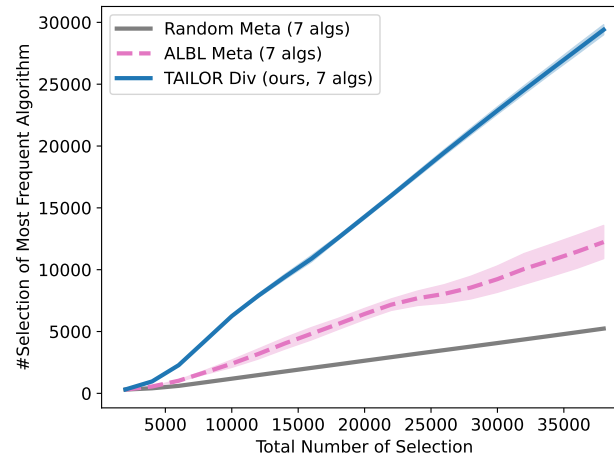


Figure 18. CIFAR-10, 2 Classes, Number of Pulls of The Most Frequent Selection

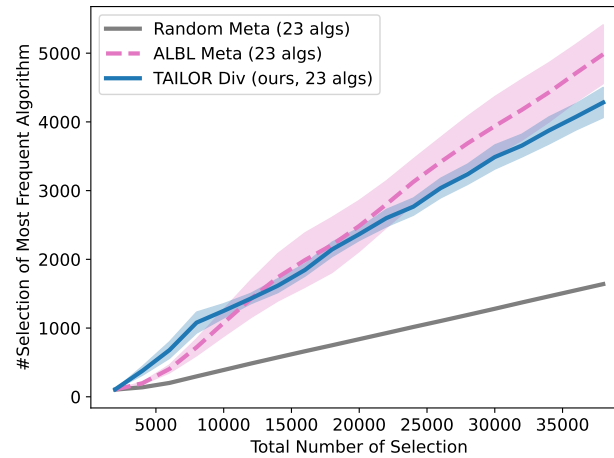


Figure 19. CIFAR-100, 10 Classes, Number of Pulls of The Most Frequent Selection

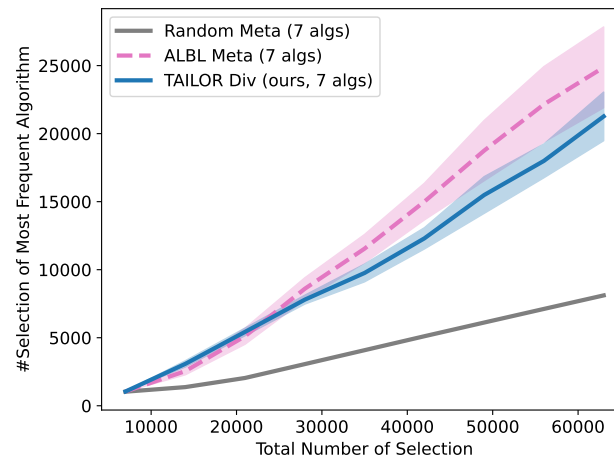


Figure 20. SVHN, 2 Classes, Number of Pulls of The Most Frequent Selection

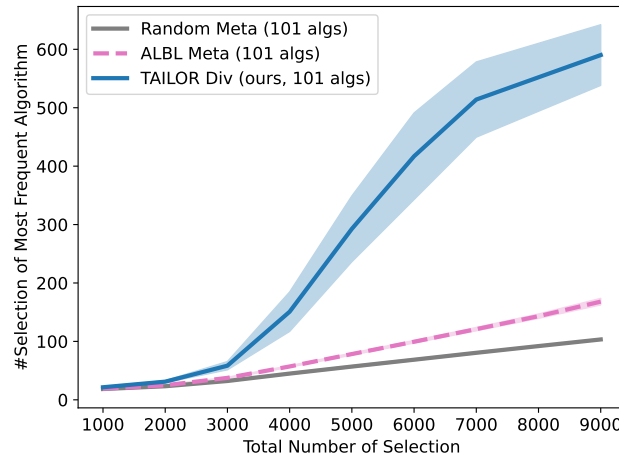


Figure 21. Kuzushiji-49, Number of Pulls of The Most Frequent Selection

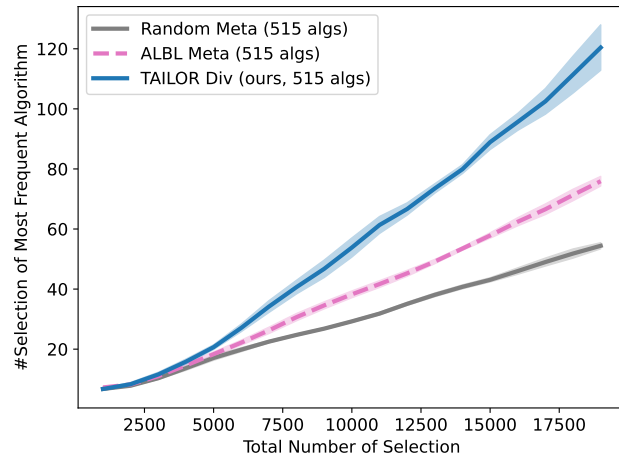


Figure 22. Caltech256, Number of Pulls of The Most Frequent Selection

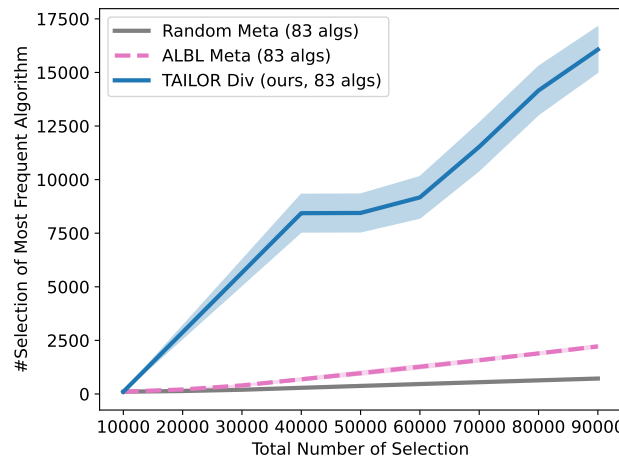


Figure 23. CelebA, Number of Pulls of The Most Frequent Selection

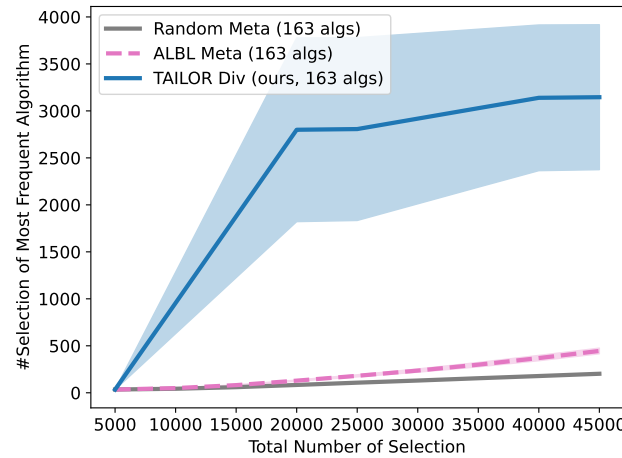


Figure 24. COCO, Number of Pulls of The Most Frequent Selection

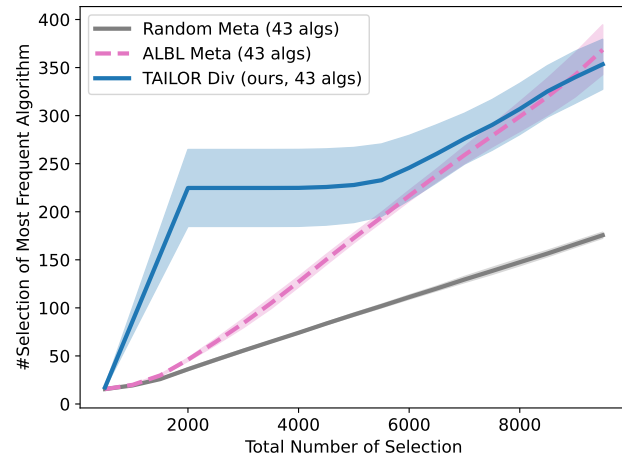


Figure 25. VOC, Number of Pulls of The Most Frequent Selection

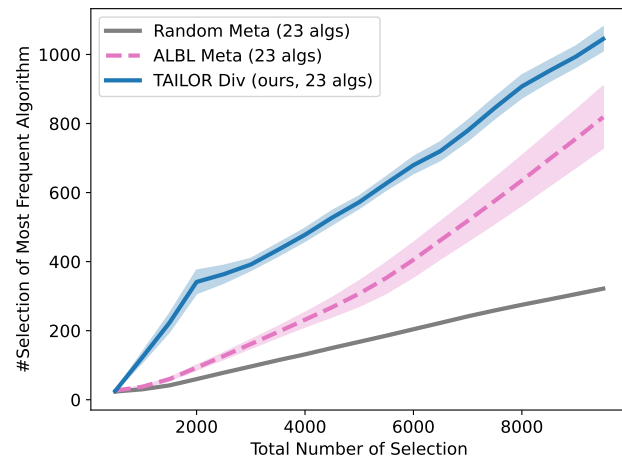


Figure 26. Stanford Car, Number of Pulls of The Most Frequent Selection